M. S. Madhusudhan
Saraswathi Vishveshwara
Molecular Biophysics Unit,
Indian Institute of Science,
Bangalore 560 012, India

Received 19 February 1998;
accepted 6 August 1998

Comparison of the Dynamics of Bovine and Human Angiogenin: A Molecular Dynamics Study

Abstract: *Molecular dynamics simulations have been carried out for 1 ns on human and bovine angiogenin systems in an effort to compare and contrast their dynamics. An analysis of their dynamics is done by examining the rms deviations, following hydrogen-bonding interactions and looking at the role of water in and around the protein. The C-terminus of bovine angiogenin moves appreciably during dynamics suggesting a better structure for ligand binding. However, we do not find any evidence of a conformation where the glutamate residue that obstructs the active site takes on a different conformation. We observe a differential hydrogen-bonding pattern in the active site regions of bovine and human angiogenins, which could have a bearing on the different catalytic activities of the proteins. We also propose that the differential binding of the monoclonal antibody toward the two proteins might be due sequential and not conformational differences. Water molecules might play an important functional role in both proteins given their subtle functional differences. A simple computation on the molecular dynamics data has been carried out to identify locations in and around the protein that are invariably occupied by water. The locations of nearly half the waters we have identified from the simulation as being invariant in bovine angiogenin occupy similar locations in the bovine angiogenin crystal structure. The positions of the waters identified in human angiogenin differ considerably from that of bovine angiogenin.* © 1999 John Wiley & Sons, Inc. Biopoly 49: 131–144, 1999

Keywords: *human and bovine angiogenin; molecular dynamics; rms deviation; loop structure; active and binding sites; invariant waters*

INTRODUCTION

Angiogenin is a 14 KD monomeric protein implicated as an inducer of blood vessel formation.[1] Though the mechanism by which this protein effects angiogenesis is far from clear, it is structurally and sequentially well characterized because of its homology to bovine pancreatic ribonuclease[2] (RNase A). It also shows RNase activity albeit 10^5 times weaker (in terms of specificity constant) than native RNase A[2]. Significantly, this weak activity is essential although not sufficient for angiogenesis. A dual site model for angiogenesis, based on biochemical evidences,[3] proposes that along with the RNase active site an endothelial cell-binding site is also vital for the activity of the protein. These two regions of the protein are now identified in the crystal structures of human angiogenin (HAng) and bovine angiogenin (BAng).[4,5] Figure 1 is a ribbon representation of BAng with the different regions labeled.

Correspondence to: Saraswathi Vishveshwara; email: sv@mbu.iisc.ernet.in
Contract grant sponsor: DST
Contract grant number: SP/SO/D44/93

CCC 0006-3525/99/020131-14

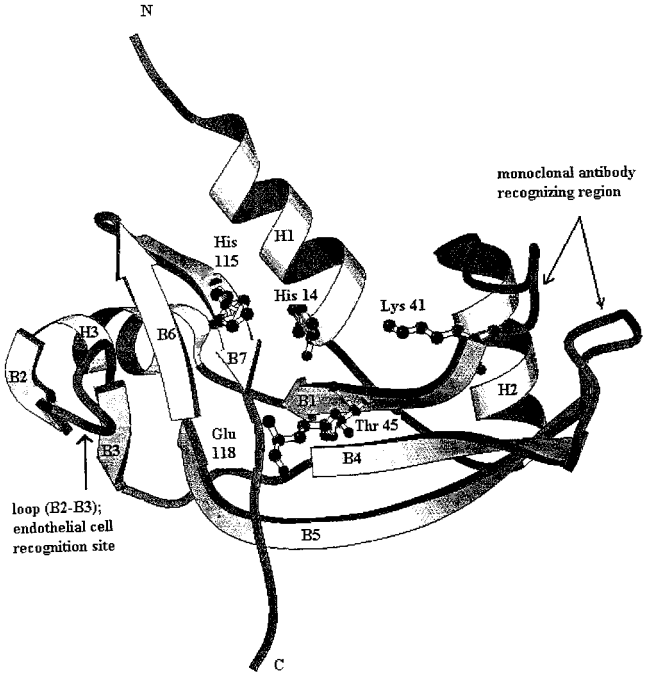

FIGURE 1 MOLSCRIPT[38] rendering of bovine angiogenin. The helices and strands are labeled along with the loops B2–B3 and B4–B5, which are biologically important.

The RNase A active and binding sites in angiogenin are fairly well conserved, but this region has two major differences. The side chain of E118 in BAng and that of Q117 in HAng are in a position that obstructs the binding of the first pyrimidine base of substrate RNA.[6] The loop connecting strands 2 and 3 is devoid of the disulphide bridge found in this region in native RNase A. This loop in RNase A has the residue N71, which has been shown to be crucial for the binding of the second nucleotide base of substrate RNA.[7] There is no equivalent of N71 in angiogenin. These differences seem to explain the low RNase activity of the protein. It is also suggested that substrate binding will be facilitated only after some conformational changes are effected.[4] Such conformational changes have not been observed in the nmr solution structure of bovine angiogenin[8] and structures of ligand-bound angiogenin are not available as yet. Another important loop in angiogenin is the one connecting strands 4 and 5 (residues 85–92 in HAng and 86–93 in BAng). It has been shown that the monoclonal antibody raised against HAng binds to this region of the protein,[9] which has very little relative affinity toward BAng. It has been postulated that the sequential difference in this region of the two proteins probably makes them take on different local conformations.[4]

Molecular dynamics (MD) simulations supplement experimental studies by providing details at an atomic scale. It is a powerful tool to study conformational flexibility and the dynamics of proteins.[10,11] In this study we have carried out 1 ns simulations of HAng and BAng, starting from their crystal structures and compared the dynamics of the two proteins. Further, the RNase A active and binding sites of the two proteins are compared with that of native RNase A. The significance of dynamics of biologically important loop regions are investigated. We have also attempted to analyze the positions in and around the protein that are invariably occupied by water. Significant importance is attached to "invariant" waters identified by x-ray crystallography from the point of view of protein stability and chemistry.[12] In this study we propose a simple computation by which the analysis of MD simulations could yield information on the location of invariant waters.

METHODS

Simulation Protocol

The simulations of bovine and human angiogenins were carried out using the AMBER 4.1 suite of programs.[13] The starting models for the two proteins were their crystal structures at 1.5 and 2.4 Å resolution, respectively[4,5] [Protein Data Bank (PDB) entries[14] 1AGI and 1ANG]. These structures were modeled using the all atom force field[15] and were solvated using TIP3P[16] waters. Waters upto a distance of

6.9 Å from the protein surface were retained. The amount of 2555 molecules of water-solvated HAng in a rectangular box with dimensions (54.67 × 47.50 × 44.00 Å) and 3243 water molecules solvated BAng in a rectangular box with dimensions (56.42 × 55.80 × 43.10 Å). The total number of atoms in HAng and BAng were 9628 and 11741 respectively. The amino acids arginine and lysine were protonated, while Glu and Asp carried a net negative charge. All histidines were protonated at both the $N^{\varepsilon 2}$ and $N^{\delta 1}$ positions except H14 (H13 in HAng), which was protonated at the $N^{\varepsilon 2}$ position only.[17]

The two systems were then subject to 1000 steps of energy minimization, where the first 200 steps were of the steepest descent method and the rest were using the conjugate gradient algorithm. The molecular dynamics that was subsequently performed on the energy-minimized system consisted of an equilibration phase of 20 ps followed by free dynamics for 1 ns. During equilibration, the system was coupled to a heat bath at 100 K for 4 ps, at 200 K for the next 4 ps, and finally at 300 K for a further 12 ps. During these 20 ps the system was coupled to a heat bath with a coupling constant = 0.1 ps.[18] The coupling was then removed and free molecular dynamics was done for 1 ns on both systems. The SHAKE algorithm[19] was used to constrain bond lengths, which facilitated the usage of 2 femtoseconds as one time step of integration. A constant value of 1 was used for the dielectric constant. The Particle Mesh Ewald sum (PME) was used to calculate electrostatic interactions,[20,21] utilizing a cubic B-spline interpolation order. The size of the grid sides was chosen to be products of 2, 3, and 5, to facilitate fast Fourier transforms. The grid spacing was ~ 1 Å. Periodic boundary conditions were applied. Nonbonded interactions were evaluated using a residue based list with a cutoff of 12 Å, updated every 25 steps. Coordinates were stored at 1 ps intervals. Rotational and translational motion of the protein was removed once every 5 steps. Velocities were rescaled every 2 ps to get the system temperature back to 300 K only if the temperature had deviated by more than 10 K from the set temperature.

The simulations were carried out using a Silicon Graphics Power Challenge Machine with 6 central processing units (CPUs) using the parallel version of the SANDER module of AMBER.

Analysis

The rms deviation (RMSDs) of the simulation structures with respect to a reference structure were found out using the superposition and least square method of Kearsley.[22] For Hydrogen-bond detection, the acceptor–donor distance was considered if it was less than 3.5 Å, where the hydrogen–acceptor distance was no greater than 2.8 Å. Surface-accessible area was found using the program of Lee and Richards.[23] The radius of the probe used was 1.4 Å.

WATER ANALYSES

The waters around the protein are analyzed for water visits, stationary waters, and invariant water positions. Protein structures are extracted from the simulation data at 10 ps intervals. The choice of the time interval is based on the mobility of bulk water of the simulation, which will diffuse through a distance of ~ 2.8 Å in the given time.

To study water visits a method similar to the one adapted by Brunne and co-workers was used.[24] Water molecules that came within the first hydration shell that was defined as a distance of 3.5 Å from a polar protein atom were counted as having made a visit. This analysis indicates how often a protein atom is hydrated. Further, if the same water molecule is in the first hydration shell for at least half the simulation time (i.e., in 50 of the 100 extracted structures), it is labeled as stationary.

The invariant water positions are analyzed as follows. The extracted structures from the simulation are all superimposed on a given reference structure. Only water molecules that hydrate the protein in the first hydration shell in all the extracted structures are retained for computation. This assembly is then enclosed in a cubical box of side 160 Å, with the protein molecule (radius of gyration ~ 15 Å) occupying the center. The box is compartmentalized into smaller cubical grids, each of side 1.6 Å. This ensures that the longest distance inside the grid, i.e., the diagonal is ~ 2.8 Å, the minimum distance of separation between two water molecules (obtained from radial distribution calculation). The first hydration shell water occupancy of the cubical grids is checked. On an average the occupancy is around 1.5 from the 100 structures we get in a 1 ns simulation. We have contoured for boxes that have an occupancy of 11 or more. This number is empirically fixed such that we have data on about 100 waters. When boxes are being contoured for this occupancy number, waters in neighboring boxes are also taken into consideration if they lie within 2.8 Å of the water in the original box. This is done to free the method of discrepancies arising from the arbitrary location of the boxes. Of these identified waters only those are chosen that make bridging interactions with two or more protein atoms.

Analyses similar to the one described here have been carried out earlier on proteins[25] and on simulations of nucleic acid structures.[26–28] Our method is closest to approach of Cheetam and Kollman.[26] A rigorous Monte Carlo method has also been reported recently to identify invariant water locations in proteins.[29] Our simple, approximate method takes much lesser CPU time for the analysis.

All analysis done on the simulation structures were done using programs developed in our laboratory, written in FORTRAN77. The dihedral angle trajectories were plotted using MATLAB and the other plots were generated using SIGMAPLOT. The C^{α} traces were done on the interactive graphics package INSIGHT made by BIOSYM, Inc.

RESULTS AND DISCUSSION

The average values of potential energy in the two systems were −28,500 and −35,300 kcal/mol with a fluctuation of less than 1%. The average simulation

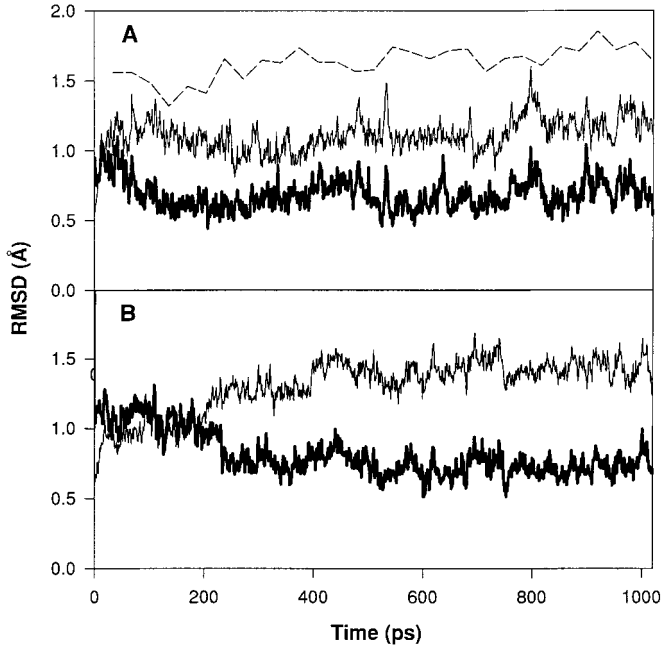

FIGURE 2 The RMSD trajectories of BAng (A) and HAng (B). The dark line in A represents the RMSD with respect to the ⟨MD⟩ structure. The thin line is that with respect to the minimized structure and the broken line is that with respect to the ⟨nmr⟩ structure.

temperature in both systems was around 306 K with a fluctuation of 3%, indicating that the system was well equilibrated.

The main chain RMSD trajectories shown in Figure 2 indicate that the conformations adopted during dynamics were close to the starting structures. In HAng the structures deviate from the minimized structure by about 1.2 Å and from the ⟨MD⟩ structure (averaged MD structure) by about 0.7 Å. The BAng structures deviate from their starting and ⟨MD⟩ structures by 1 and 0.6 Å, respectively. In HAng, there is an increase in the RMSD for about 300 ps. This change is gradual and does not correspond to any drastic conformational change in the protein. Figure 2A also shows the RMSD of the simulation structures of BAng from the ⟨nmr⟩ (averaged nmr structure) structure. The values range from 1.5–1.8 Å. The RMSD of the ⟨nmr⟩ structure from the crystal structure also lies in this range (~ 1.8 Å).

Figures 3A and 3B show the residue wise main chain rms fluctuations of BAng and HAng about their ⟨MD⟩ structure. The rms fluctuations are an indication of the conformational flexibility of the residues that make up the proteins. In both systems, loops fluctuate the most. In HAng, the loops lying between H1 and H2, B2 and B3, and B4 and B5 (Helix 1: helix 1, etc.; B1; strand 1, etc.) and the second helix have large fluctuations. On the other hand, the BAng system has large fluctuations only in the H2–B1 and B4–B5 loops. The C-termini of the two proteins also show different dynamic behavior. The 3_{10}-helical C-terminus of HAng shows very little fluctuation as compared to the unstructured C-terminus of BAng. The main chain rms fluctuations of the nmr structures with respect to (w.r.t.) the ⟨nmr⟩ structure is coplotted in Figure 3A. It is interesting to note that the deviations of the nmr structures from their average is qualitatively the same as that of the simulation structures from their averaged structure. The large RMSD of the C-terminus of BAng w.r.t. the crystal structure (Figure 3A) is significant from the point of ligand binding. Our preliminary docking studies reveal that the ⟨MD⟩ structure is sterically better than the crystal structure for ligand binding.

Loop Structures

In the crystal structure of HAng, the loop connecting H2 and B1 has a peptide unit (S37—P38) with an ω torsion angle value of 96.94°. This value is close to the peak of the energy barrier of the ω torsion angle and is therefore unrealistic. On minimizing the protein, this value changed to 125°. The value fluctuated around 150° for the first 250 ps of the simulation, after which it took on a *trans* conformation and was stable in that conformation for the rest of the simulation. The corresponding region in BAng is a *cis* peptide unit involving R38 and P39. The stabilization of this *trans*

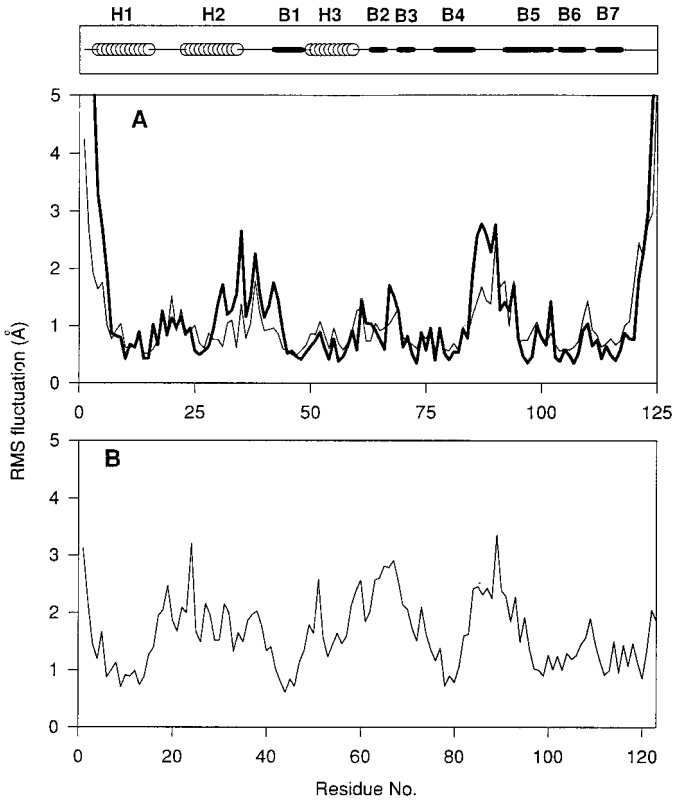

FIGURE 3 Residuewise rms fluctuation with respect to the ⟨MD⟩ average structure of BAng (A) and HAng (B). The bold line in A is the rms fluctuation of nmr structures with respect to the ⟨nmr⟩ structure.

peptide unit does not advent any structural disparity in this region. Comparing the C^{α} traces of BAng and HAng crystal structures and ⟨MD⟩ structures superimposed in Figures 4A and 4B do not show any significant difference in this region. This also accounts for the large rms fluctuation of this loop region in HAng, where the stabilization of the *trans* conformation leads to readjustments of neighboring residual torsion angles so that the structure is locally maintained similar to what we see in BAng.

The loop connecting strands B2 and B3 has been identified as a part of the endothelial cell receptor binding site.[30] This region could also play a role in recognizing and binding to RNA ligands. Though this region is vital for the functioning of the protein it is not well conserved among the angiogenins of various organisms.[31] This loop takes on different conformations in HAng and BAng, as is evident from Figure 5, which shows trajectories of the backbone torsion angles ϕ and ψ of this region. Except the loop residues R67, G68, and D69 in BAng, and R66, E67 and N68 HAng, the other residues whose ϕ–ψ trajectories are shown were the same in the starting structures of both systems. After about 250 ps the ψ of H65 and the ϕ and ψ of R66 of HAng change significantly. Another set of significant changes in torsion angles occurs after about 500 ps where the ψ of P64 and the ψ of N68 along with the ϕ of H65 change. The ψ values of N63 and that of E67 also change but unlike in the other cases the transition is gradual. One reason for the relative rigidity of BAng in this region could be the hydrogen-bonding interaction of the R67 residue with D117 of the C-terminus (see Table I), which is also for part of the time supplemented by a water-mediated hydrogen bond. The observed changes in the conformation of this loop supplement the crystallographically observed differences in this region of the two proteins. The conformation of the loop, however, is different from the crystal structure during dynamics. This could be of some importance during identification and binding of the second nucleotide of substrate RNA.

The backbone of the loop connecting strands B4 and B5 scan similar regions in torsional angle space in both proteins as inferred from Figure 6. The glycine doublet contributes to a lot of main chain fluctuation, yet the torsional angle space sampled by this region in BAng and HAng are similar. This region in HAng is

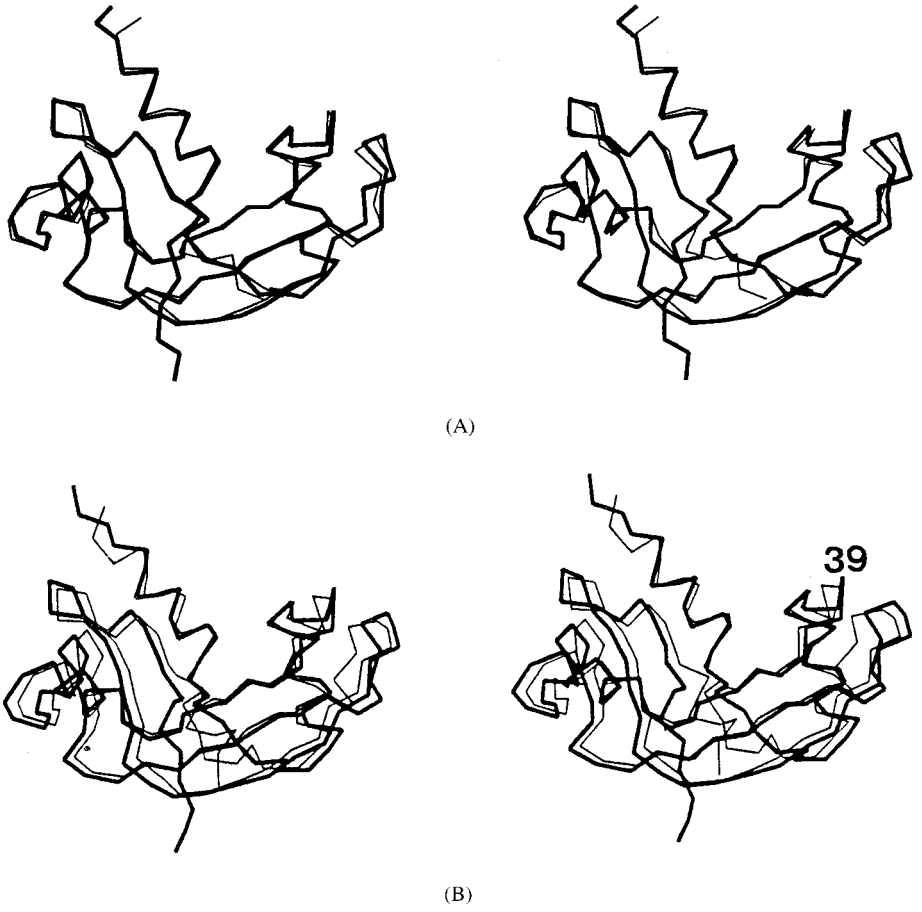

FIGURE 4 Superimposition of the C^{α} traces of human and bovine angiogenins. (A) Crystal structures. (B) ⟨MD⟩ structures.

implicated in binding to a monoclonal antibody, toward which BAng has very low affinity. Significantly, the presence of nonconservative differences in the sequences of the two proteins in this region (K85 for H84, S89 for P88, and R90 for W89) does not alter the conformation of the backbone. The difference in affinity of HAng and BAng toward the antibody might therefore be a manifestation of the sequential difference in this region and not due to any backbone conformational change as suggested in the crystal structure report.[4]

Active and Binding Sites

The residues in the RNase active site are seen to be extensively hydrogen bonded among themselves in the crystal structure. Some of these interactions are retained during the course of the simulation while others are broken, some giving way to newer interactions. Table I lists these interactions.

The side chains of the obstructive E118 in BAng and Q117 in HAng make H bonds with T45 and T44, respectively. These H-bond interactions are, however, dissimilar (see Table I). In HAng the main chain N of T44 interacts with the side chain of the Q117 residue whereas in the BAng it is a T45—Q117 side chain–side chain interaction. These hydrogen bonds are retained for the length of the simulation. In addition to these interactions the E118 in BAng also has stable side chain–side chain interactions with R43. This could have implications on the differential activity of the two proteins.

The active site residues in BAng show very little deviation from its position relative to RNase A (PDB code 7RSA) as evaluated by rms fluctuations. The catalytic histidines (H13/H14 and H114/H115) from the MD simulation structures were superimposed on those of the crystal structure of RNase A. The histidines only fluctuate from the RNase position by about 0.3 Å during the course of simulation. The ring of the catalytic H114 in HAng flips whereas the corresponding H115 of BAng does not (Figure 7). This leads to a higher value of RMSD for the catalytic histidines ($\sim$ 1.5 Å) in the case HAng. Crystallographic and nmr

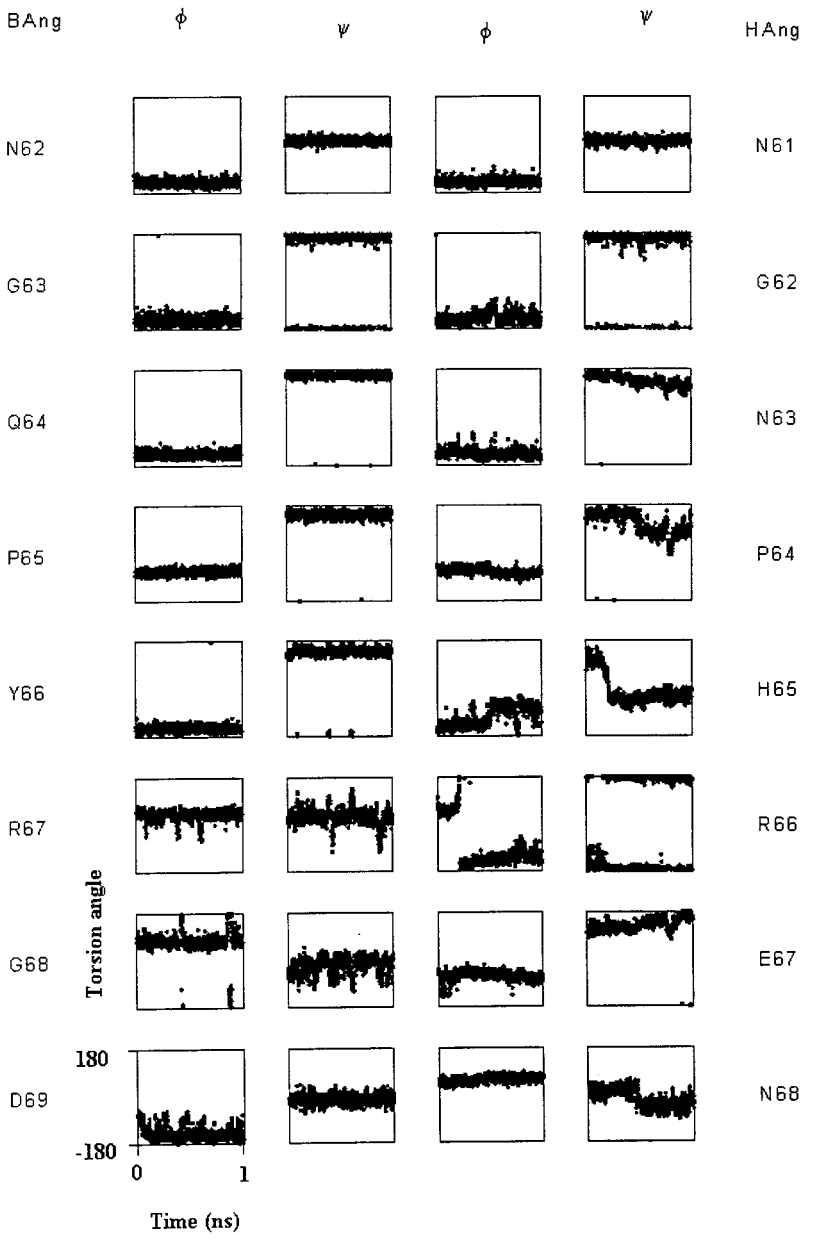

FIGURE 5 The backbone torsion angles of the region encompassing the loop B2–B3 in BAng and HAng.

work on RNase A have shown that the histidine 119 ring in RNase A also flips in some cases to an alternate conformation.[32,33] This conformation has been shown to be vital for docking nucleotide ligands onto RNase A.[34] In HAng and BAng, the main chain of these catalytic Histidines in both proteins have water-mediated hydrogen-bonding interactions with A106 and G107, respectively (Table I). These interactions ensure the positional stability of the histidine main chains. Another set of important interactions that have implications to ligand binding are the ones that H13 (H14 in BAng) makes with residues in the region encompassing residues 45–47 in the crystal structure, especially in that of BAng. This region is shown to bind to the first nucleotide base of the ligand, single stranded RNA.[35] The breaking of these interactions during the simulation could be an indication of the dynamics of the protein that would facilitate ligand binding.

The side chain of the other catalytically important residue K40 (K41 in BAng) fluctuate to a large extent (0.8 Å) with respect to the native RNase position,

Table I Intraprotein Hydrogen Bonds in Human and Bovine Angiogenin[a]

Human Angiogenin							Bovine Angiogenin						
Donor		Acceptor		Distance (Å)			Donor		Acceptor		Distance (Å)		
Res	Atom	Res	Atom	X-Ray	Min.	⟨MD⟩ (RMSD)	Res	Atom	Res	Atom	X-Ray	Min.	⟨MD⟩ (RMSD)
R5	NH2	E108[b]	Oε2	—	2.75	2.58(1.)	R6		E109[b]	Oε2	2.83	2.72	2.66(.8)
H13	O	T44	O	—	3.35	—	H14	O	I47	N	2.74	—	—
								Nδ1	T45	O	2.75	3.48	—
K40	O	Y94[b]	OH	2.91	2.68	2.62 (.2)	K41	N	L36	O	3.10	—	—
	Nζ	N43	Oδ1	2.94	2.78			O	Y95[b]	OH	2.76	2.69	2.79(.3)
								Nζ	N44	Oδ1	3.10	2.81	—
T44	N	Q117	Oε1	3.12	2.96	2.92 (.3)	T45	N	E118[b]	Oε2	2.90	3.47	
	Oγ1	T80	Oγ1	2.72	2.84	2.85 (.3)		Oγ1		Oε1	2.74	2.54	2.80(.8)
H114	N	A106[c]	O	3.61	—	—	H115	N	G107[c]	O	3.21	—	—
	O		N	2.85	2.94	2.96 (.3)		O		N	2.84	2.92	2.90(.2)
D116	Oδ1	S118	Oγ	2.76	—	2.60 (.7)	D117	N	V105	O	3.11	—	—
	Oδ2		Oγ	2.96	2.60	2.90 (.7)		Oδ1	S119	Oδ1	2.64	—	—
								Oδ1		N	2.99	—	—
								Oδ1	R67[b]	NH1	—	2.75	2.92(.5)
								Oδ2		NH2	—	2.84	2.92(.6)
							E118	O	R43	NH1	2.91	2.88	—
								Oε1		Nε	3.38	2.81	3.13(.5)

[a] The three distances reported for HAng and BAng correspond to the distance of the acceptor from the donor in the x-ray structure, the minimized structure, and the ⟨MD⟩ structure. The rms deviation from the ⟨MD⟩ value is given in brackets in Å units.

[b] Hydrogen bonds bolstered by water-mediated hydrogen bonds during dynamics.

[c] Hydrogen bonds replaced by water-mediated hydrogen bonds during dynamics.

even as its backbone O is H bonded to the OH of Y94 (Y95 in BAng). This H bond seems to hold the K40 (K41) in position. In a recent study on RNase A it was shown that a mutation in the Y95 equivalent, Y97, led to a 20% decrease in enzymatic activity.[36]

The residues identified as forming part of the site that binds to the second nucleotide, R5 and E108 (R6 and E109 in BAng),[37] are hydrogen bonded to each other during the course of simulation. These hydrogen bonds are supplemented by water-mediated hydrogen bonds. This hydrogen bond was observed only in the crystal structure of BAng and not in that of HAng.

Water Around the Proteins

The role of water molecules in stabilizing protein structure is well known. Our analysis on the solvent water has been done on simulation structures extracted after every 10 ps of dynamics. The residence time of water molecules in the first hydration shell, if not ensnared in some local potential energy pit, on an average is of the order of 10 ps, a range similar to the one reported in an earlier study.[24] One nanosecond is a time scale that should give us statistically significant information on events that occur on a time scale of 10 ps. Further, Figure 8 shows the plot of surface accessibility coplotted with water visits to the residues of the protein. In both proteins the profiles of the two coplots look similar, indicating that there are no anomalous effects in play. The water visits profile also agreed qualitatively with the nmr data on hydrogen exchange.[8]

Stationary Water Molecules. A residence time criterion as elucidated in the methods section is used to identify stationary water molecules. Stationary waters adorn different locations around the protein. These waters are those that stay in the first hydration shell of the protein for a long time (at least half the simulation time in this case). Predominantly their interactions are only with a few protein groups but they all tend to roll around. Not all the stationary waters fit into the invariant class even though at some point of time they may occupy an "invariant" location. The location of some of the stationary waters can also be deduced from Figure 8, which is the coplot of water visits and surface accessibility. The regions where a high surface accessibility corresponds to a relatively lower

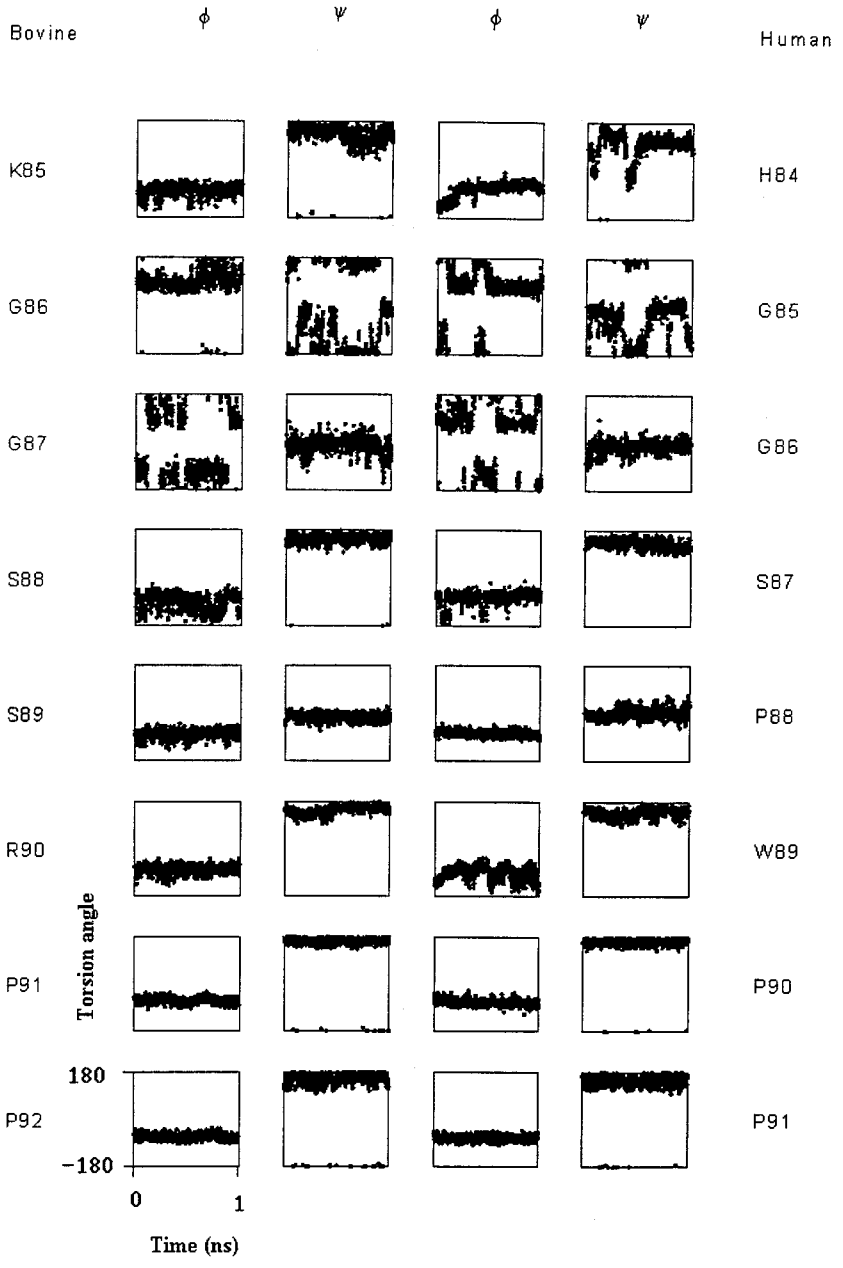

FIGURE 6 The backbone torsion angles for the region between strands B4 and B5 in BAng and HAng.

number of visits are regions that are likely to have stationary waters. These regions in BAng correspond to the loop regions between B4–B5, B3–B4, B2–B3, and the C-terminus. In HAng, by contrast, the regions where stationary waters are found are in the loop regions between H1–H2, H2–B1, and B4–B5. In BAng some of the active/binding site residues like T45 have interactions with the stationary waters. This is not so in HAng. The only common protein–stationary water bridging interactions in the two proteins are those that bridge the loop B6–B7 to the first helix. It is surprising that the stationary water positions in the two proteins are different. It can be explained by the fact that the regions where the waters are stationary in the two proteins have different amino acid compositions, which could lead to different local potential energy profiles.

Invariant Water Positions. We label water positions as invariant based on positional invariance of a water

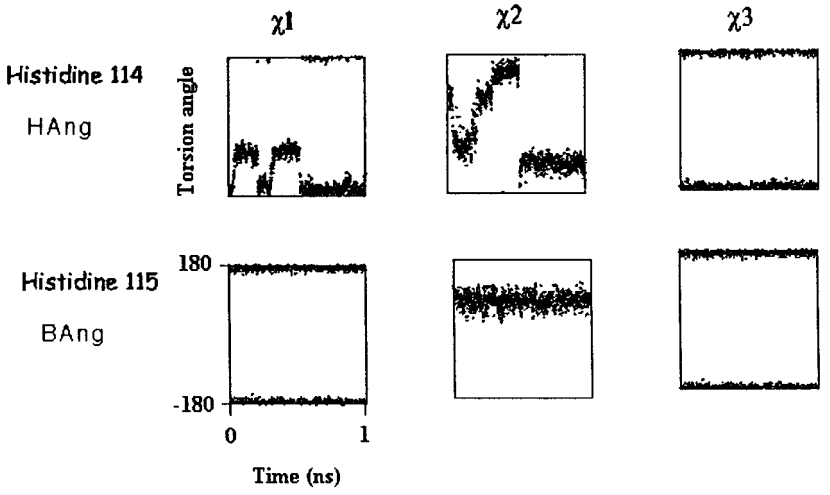

FIGURE 7 Side chain torsion angles of catalytic histidine 114 from HAng and histidine 115 from BAng.

molecule that bridges two or more protein atoms. A comparison of the locations of the invariant waters identified from our simulations on BAng with those of the crystal structure (Figure 9A, Table II) agree very well even though the crystal structure waters were not used in the simulation.

Nineteen waters in the crystal structure bridge atoms of 2 or more residues (Figure 9A). The invariant waters obtained from MD simulation analyses are compared to these (Table II). Six of the 14 waters identified as invariant during the BAng simulation have the same interaction as waters in the crystal

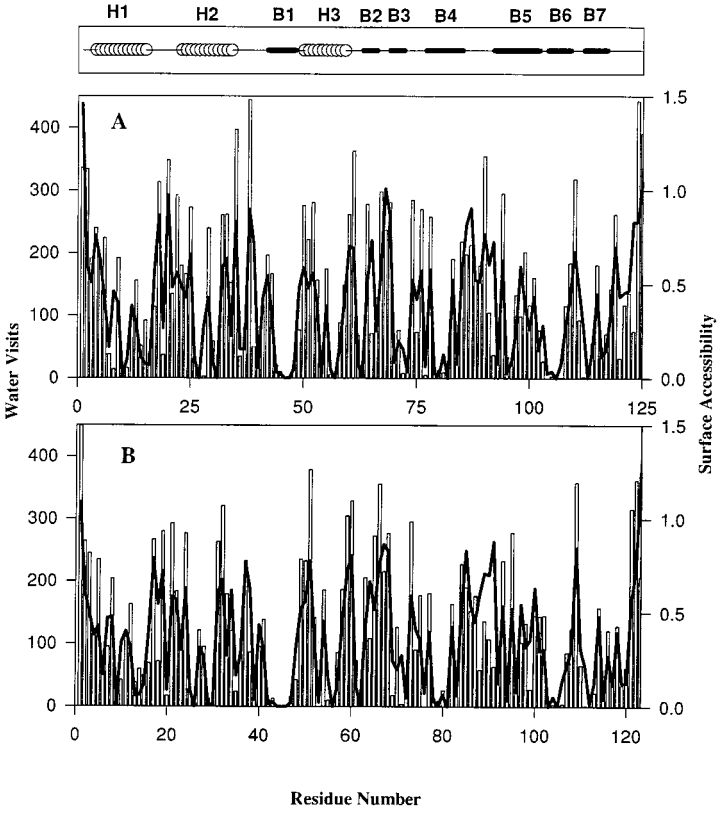

FIGURE 8 Surface-accessible area (thick line) normalized by the area of X—Gly—X, coplotted with the number of water visits made residuewise in BAng (A) and HAng (B).

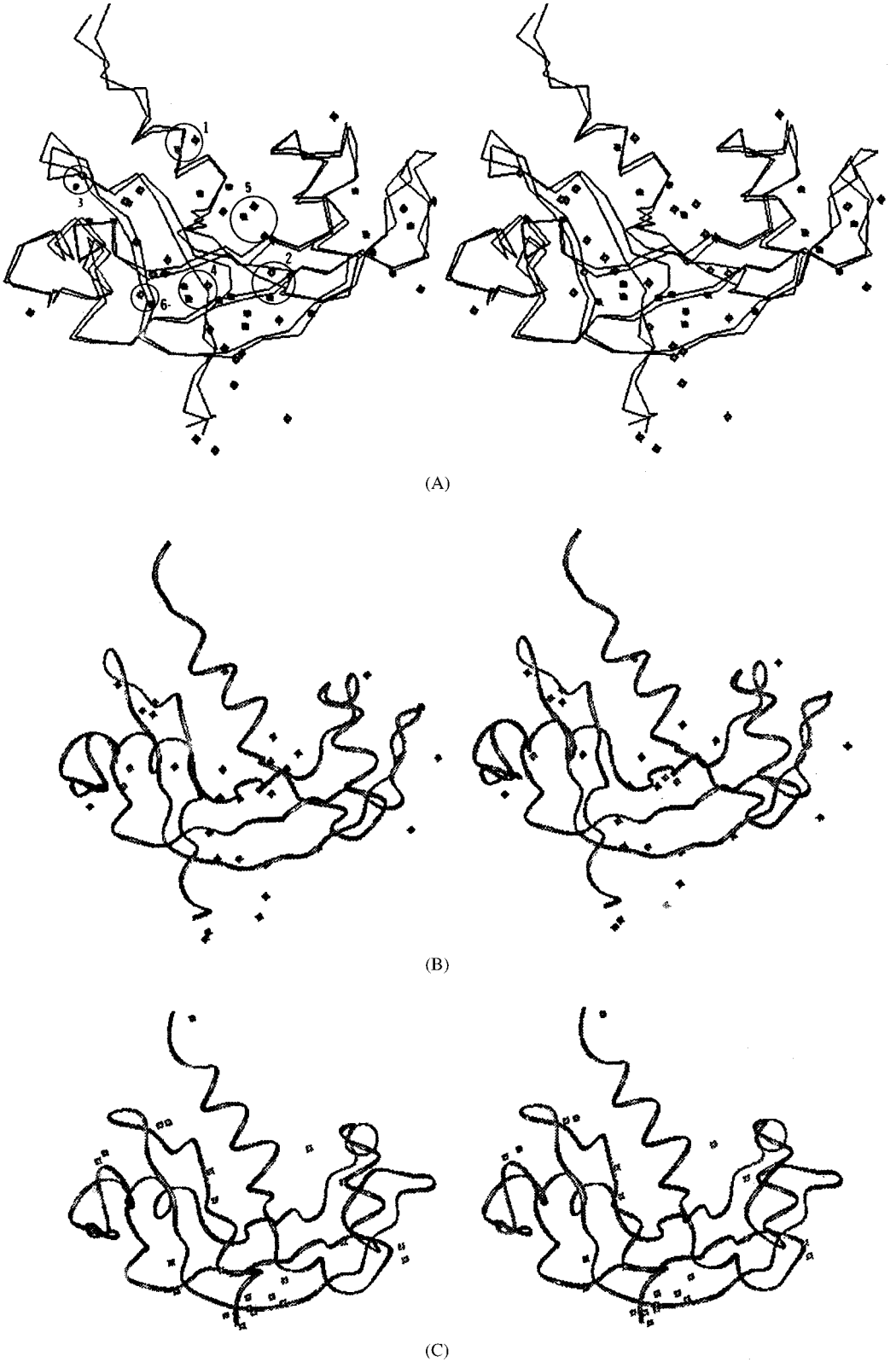

FIGURE 9 Stereo plots of invariant waters shown on C^{α} traces of bovine and human angiogenins. (A) A representative snapshot from MD simulations of BAng superimposed on its crystal structure. The invariant water positions common to the simulation and crystal structure are encircled and numbered (as listed in Table II). The lighter lines and circles represent the BAng MD snapshot C^{α} trace and invariant watermolecules while the darker lines and circles are for the BAng crystal structure. (B) A representative structure of the invariant water positions in bovine angiogenin. (C) A representative structure of the invariant water positions in human angiogenin.

Table II Invariant Water Bridges Common to BAng Crystal Structure and the MD Structures of BAng and HAng[a]

Interacting Water Number	Interacting Protein Group	Distance in Crystal Str. (Å)	Distance in Bang Sim. (Å)	Distance in Hang Sim. (Å)
1	O Arg 6	2.77	2.70	
	N Phe 10	3.34	3.13	
	O Val 114	2.90	2.81	
2	O His 48	3.00	2.73	
	N Gln 78	2.94	3.13	
3	O Asp 69	2.85	2.61	3.22(OD1)[b]
	N Cys 108	2.98	2.89	2.83 (O)
4	NH2 Arg 102	2.56		
	N Val 105	3.00	2.94	
	O Val 105	3.24	3.50	3.31
	O Asp 117	2.80	2.62	3.23 (N)
5	NE2 Arg 43	3.48	3.21	2.73
	NH1 Arg 43	3.31	3.02	
	O Glu 118	3.08	2.98(OE1)	3.41
6	NH1 Arg 67	3.45	3.08	
	OD2 Asp 117	2.94	2.61(OD1)	
	OG Ser 119	3.27	3.48 (N)	
7	O Arg 22	—	3.02	2.73
	OG1 Thr 80	—	2.83	—
	OE2 Glu 99	—	2.79	3.36 (N)

[a] The reported protein–water distances are averages of protein–water interactions from different structures where these bridging interactions exist.

[b] Given in parentheses are the interacting protein atoms of the corresponding residue in the MD simulations that are different from those in crystal structure.

structure. On the other hand, only 3 of the 15 from the HAng simulation have similar interactions to those found in the BAng crystal structure. These three waters are common to the two simulations. There is one other common water from the two simulations that is not found in the crystal structure (bridging residues 21 and 98 in HAng). All waters that have been picked out as having the interactions in the MD and crystal structures are within 2 Å of each other when the interacting residues and the water alone are superimposed (i.e., they fall within the same box). Figures 9B and 9C show a representation of these waters on a representative MD snapshot of the C^{α} trace. The number of waters exceeds the numbers of 14 and 15 in BAng and HAng to accommodate the several spatial positions in which these waters are present during dynamics, retaining the same interactions.

It is interesting to note that a number of invariant waters bridge the backbone atoms, perhaps contributing to further strengthening of the protein structure. Three invariant waters common to the BAng crystal structure and the two simulations (see Table II) seem to bridge a complete domain of the protein. Further, invariant waters and water bridges connect the loop between strands B2 and B3 to the C-terminus in both proteins. This is a significant interaction as this loop and its positioning is very important for the biology of the protein. Here it must be emphasized that in BAng there is a protein–protein interaction as well, between these two regions (R67 and D117). Invariant waters are also found in and around the RNase active and binding site regions in both proteins. The role of these waters has been analyzed with some rigour by previous studies.[12] Two other important regions of the protein that are bridged by invariant waters are the loops (H2–B1) and (B4–B5). The importance of this bridging interaction stems from the fact that the monoclonal antibody raised against the HAng binds to these two loop regions of the proteins (Figure 1). That the two loops in both proteins are held together by waters clearly supplements our claim in an earlier section that it is the nature of the side chains and not the loop conformations in the two proteins that hold the key to differential binding to the antibody.

The other invariant waters in the two proteins occupy different locations. Interestingly these other waters interact with residues on the surface of the

protein. But the interactions are with only partially exposed atoms of the exposed residues.

SUMMARY

BAng and HAng have 125 and 123 residues, respectively, and are 64% sequentially homologous to each other. The two structures differ significantly in the C-terminus region and in the region of the loop connecting strands 2 and 3. No major alteration happens to the overall structure during the course of simulation. The ω(37–38) torsion angle, which was reported to take a value of 96.94° (close to the peak of the peptide torsion angle barrier) in the crystal structure of HAng, takes a *trans* orientation in our simulation. A higher resolution crystal structure may resolve the value of this parameter. The corresponding ω(38–39) of BAng was *cis* in the crystal structure and remained in that orientation throughout the simulation.

There are significant differences in the dynamics of the two angiogenins. The essence of this is captured in the varying loop conformational versatility of the two systems. Further, the residues implicated in binding to a monoclonal antibody in HAng (85–92) explore the same conformational regions as their counterparts in Bang (86–93), toward which the antibody has a much lower affinity, suggesting that the nature of the residues is crucial for antibody recognition. This is in contrast to what the crystal structure studies report. The regions identified as the endothelial cell receptors in the two proteins (around 61–69) do not conform to the same backbone orientation, indicating that this might lead to different means of cell receptor recognition in the two proteins as well as differential substrate recognition. Additionally, this might also have implication in the ligand specificity of the two proteins as this region also encompasses the B2 binding residues. In the crystal structure of HAng, the C-terminus was an ordered 3_{10}-helix whereas it lacks secondary structure in BAng. Consequently during dynamics, fluctuations in this region is less in HAng compared to that of BAng. Interestingly, however, this region of BAng (D117) forms a stable hydrogen bond with R67 of the loop responsible for endothelial cell recognition.

The backbone of the C-terminus of BAng deviates noticeably from the crystal structure during simulation, which seems to be a better structure for ligand interaction. However, the side chains of E118 (Q117) form stable hydrogen bonds with T45 (T44), still obstructing the perfect positioning of the nucleotide base of the ligand. Interestingly, E118 in BAng is held in place by tighter interactions than Q117 in HAng. This might play a role in differential activities of the two proteins. The hydrogen-bond interaction between H14 and T45 observed in the crystal structure of BAng is broken during dynamics, which possibly may facilitate ligand binding. Both the catalytic histidines are in the same location as in RNase A except for H114 in HAng, which undergoes a ring flip. This is not unusual as earlier studies have shown, and may be an important conformational change for catalysis or ligand binding.

A procedure to identify the location of invariant water positions has been developed by generating grids around the protein molecule. Some of the invariant water bridges analyzed from MD structures of BAng correspond well with those found in the crystal structure of BAng. Although some of these waters are also present in the HAng simulation, there is a cognizable difference in the invariant water positions of the two proteins. This suggests a role for water in the differential activities of the two proteins.

We thank the Supercomputer Education Research Centre (SERC) and the Bioinfomatics centre of the Indian Institute of Science for computational facilities and graphics facilities. Gautham Nadig is thanked for useful discussions. We thank one of the referees for constructive criticism on the water analysis. The work was partially supported by DST scheme no. SP/SO/D44/93.

REFERENCES

1. Vallee, B. L.; Riordan, J. F.; Lobb, R. R.; Higachi, N.; Fett, J. W.; Crossley, G.; Buhler, R.; Budzik, G.; Breddam, K.; Bethune, J. L.; Alderman, E. M. Experientia 1985, 41, 1–15.
2. Riordan, J. F. In Ribonucleases Structures and Functions; D'Alessio, G.; Riordan, J. F., Ed.; Academic Press: 1997; New York, pp 445–489.
3. Hallahan, T. W.; Shapiro, R.; Vallee, B. L. Proc Natl Acad Sci 1991, 88, 2222–2226.
4. Acharya, K. R.; Shapiro, R.; Riordan, J. F.; Vallee, B. L. Proc Natl Acad Sci USA 1995, 92, 2949–2953.
5. Acharya, K. R.; Shapiro, R.; Allen, S. C.; Riordan, J. F.; Vallee, B. L. Proc Natl Acad Sci USA 1994, 91, 2915–2919.
6. Russo, N.; Shapiro, R.; Acharya, K. R.; Riordan, J. F.; Vallee, B. L. Proc Natl Acad Sci USA 1994, 91, 2920–2924.
7. Tarragona-Fiol, A.; Eggelte, H. J.; Harbron, S.; Sanchez, E.; Taylorson, C. J.; Ward, J. M.; Rabin, B. R. Protein Eng 1993, 6, 901–906.
8. Lequin, O.; Albaret, C.; Bontems, F.; Spik, G.; Lallemand, J. Y. Biochemistry 1996, 35, 8870–8880.
9. Fett, W. F.; Olson, K. A.; Rybak, S. Biochemistry 1994, 33, 5421–5427.

10. Elber, R.; Karplus, M. Science 1987, 235, 318–321.
11. Nadig, G.; Vishveshwara, S. Biopolymers 1997, 42, 505–520.
12. Zegers, I.; Dominique, M.; Minh-Hoa, D.; Poortmans, F.; Palmer, R.; Wyns, L. Protein Sci 1994, 3, 2322–2339.
13. Pearlman, D. A.; Case, D. A.; Caldwell, J. W.; Ross, W. S.; Cheetam, T. E., III; Ferguson, D. M.; Seibel, G. L.; Singh, U. C.; Weiner, P. K.; Kollman, P. A. AMBER4.1, University of California, San Francisco, 1995.
14. Abola, E. E.; Sussman, J. L.; Prilusky, J.; Manning, N. O. Methods Enzymol 1997, 277, 556–571.
15. Cornell, W. D.; Cieplak, P.; Bayly, C. I.; Gould, I. R.; Merz, K. M., Jr.; Ferguson, D. M.; Spellmeyer, D. C.; Fox, T.; Caldwell, J. W.; Kollman, P. A. J Am Chem Soc 1995, 117, 5179–5197.
16. Jorgensen, W. L.; Chandrashekar, J.; Madura, J. D.; Impey, R. W.; Klien, M. L. J Chem Phys 1983, 79, 926–935.
17. Eftink, M. R.; Biltonen, R. L. Biochemistry 1983, 22, 5123–5134.
18. Berendsen, H. J. C.; Postma, J. P. M.; van Gunsteren, W. F.; DiNola, A.; Haak, J. R. J Chem Phys 1984, 81, 3684–3690.
19. Ryckaert, J. P.; Ciccotti, G.; Beredsen, H. J. C. J Comput Phys 1977, 23, 327–341.
20. Darden, T.; York, D.; Pedersen, L. J Chem Phys 1993, 98, 10089–10092.
21. Cheetam, T. E., III; Miller, J. L.; Fox, T.; Darden, T. A.; Kollman, P. A. J Am Chem Soc 1995, 117, 4193–4194.
22. Kearsley, S. K. Acta Cryst 1989, A45, 208–210.
23. Lee, B.; Richards, F. M. J Mol Biol 1971, 55, 379–400.
24. Brunne, R. M.; Liepinsh, E.; Otting, G.; Wuthrich, K.; van Gunsteren, W. F. J Mol Biol 1993, 231, 1040–1048.
25. Lounnas, V.; Pettit, B. M. Proteins 1994, 18, 133–147.
26. Cheetam, T. E.; Kollman, P. A. J Am Chem Soc 1997, 119, 4805–4825.
27. Young, R. A.; Jayaram B.; Beveridge, D. L. J Am Chem Soc 1997, 119, 59–69.
28. Shields, G. C.; Laughton, C. A.; Orozoo, M. J Am Chem Soc 1997, 119, 7463–7469.
29. Marrone, T. J.; Resat, H.; Hodge, N. C.; Chang, C.; McCammon, J. A. Protein Sci 1998, 7, 573–579.
30. Harper, J. W.; Vallee, B. L. Biochemistry 1989, 28, 1875–1884.
31. Bond, M. D.; Strydom, D. J.; Vallee, B. L. Biochem Biophy Acta 1993, 1162, 177–186.
32. Borkakoti, N.; Moss, D. S.; Palmer, R. A. Acta Cryst 1982, B38, 2210–2217.
33. Rico, M.; Santoro, J.; Gonzalez, C.; Bruix, M.; Neira, J. L.; Nieto, J. L.; Herranz, J. J Biomol NMR 1991, 1, 283.
34. Seshadri, K.; Balaji, P. V.; Rao, V. S. R.; Vishveshwara, S. J Biomol Str Dyn 1993, 11, 395–415.
35. Pares, X.; Noguez, M. V.; Llorens, R. D.; Cuchillo, C. M. In Essays in Biochemistry, Vol. 26; Tipton, K. F., Ed.; Portland Press: London, UK, 1991; pp 89–103.
36. Juminaga, D.; Wedemeyer, W. J.; Garduno-Juarez, R.; McDonald, M. A.; Scheraga, H. A. Biochemistry 1997, 36, 10131–10145.
37. Russo, N.; Acharya, K. R.; Vallee, B. L.; Shapiro, R. Proc Natl Acad Sci 1996, 93, 804–808.
38. Kraulis, P. J. J Appl Crys 1991, 24, 946–950.